

Correction to the Interfacial Tension by Curvature Radius: Differences between Droplets and Bubbles

Aly J. Castellanos S.,* Jhoan Toro-Mendoza, and Maximo Garcia-Sucre

Laboratorio de Fisicoquímica de Coloides, Centro de Física, Instituto Venezolano de Investigaciones Científicas (IVIC), Carretera Panamericana, Km. 11, Altos de Pipe, Caracas 1020A, Venezuela

Received: October 8, 2008; Revised Manuscript Received: January 13, 2009

In this work we analyze the behavior of the interfacial tension with the curvature radius of the disperse phase. Following the Young–Laplace deduction of the equation relating the internal pressure with the curvature radius for a fluid confined by a spherical interface, we restate the Tolman approach [*J. Chem. Phys.* **1949**, *108*, 333] to obtain an analytical expression relating the interfacial tension with the radius. We have found small differences between our results and those of Tolman for the liquid/gas (droplets) case. However, important differences between liquid/gas (droplets) and gas/liquid (bubbles) dispersions were found. In particular, the decrease in the interfacial tension of bubbles may be expected to occur for much larger curvature radii than for the case of droplets when the curvature radius decreases. A simple relation between the Tolman's δ parameter and the interfacial width is also discussed. In our calculations we have considered dispersions of droplet of water in methane and bubbles of methane in water at $T = 273.15$ K.

Introduction

Interfacial tension σ is a striking property of fluid/liquid interfaces, and it plays an important role in the fluid/liquid dispersions stability. Nowadays, nanoemulsions studies indicate unexpected deformability of the droplet surface, despite its high internal pressure predicted by the Young–Laplace equation.¹ In the seminal paper of Tolman, a correction for σ by the curvature radius r of a spherical particle was proposed.² As a consequence, a length δ was obtained defined as the separation between the surface of tension and the equimolar dividing surface, namely:

$$\delta = \frac{\Gamma}{\gamma' - \gamma''} \quad (1)$$

where Γ is the molar surface density at the boundary between the two phases ($\Gamma = 1/\omega$, where ω is the molar surface area), and γ' and γ'' are the densities of liquid and vapor phases, respectively. However, some interpretative difficulties have been reported concerning negative values for δ .³

On the other hand, most of the works focus on droplet in gas systems.^{4–7} A difficulty found when using the correction proposed by Tolman is the appearance of the term $(\gamma' - \gamma'')$ in the definition of δ for the case of bubbles dispersed into a liquid medium. This factor appears as a consequence of considering that the external pressure variation of the droplet (P_{out}) has an important contribution to the variation of the capillary pressure P_C . This idea is supported by the Kelvin equation where the vapor pressure of a liquid confined into a droplet changes according to:

$$RT \ln \frac{P_v}{P_{fs}} = \frac{2\sigma v_L}{r} \quad (2)$$

Here, P_{fs} is the vapor pressure of a liquid with flat surface, P_v is the vapor pressure with a curved surface of radius r , v_L is the molar volume of the liquid, T is the temperature, and R is the universal gas constant.

For the reasons mentioned above, the capillary pressure of a droplet is frequently defined as the difference between the internal pressure P_{in} and the vapor pressure P_v , that is, $P_C = P_{\text{in}} - P_v$. However, appreciable differences between P_{fs} and P_v have been found only for curvature radius smaller than 10 nm.⁸ On the other hand, by considering the Young–Laplace equation:

$$P_C = P_{\text{in}} - P_v = \frac{2\sigma}{r} \quad (3)$$

and taking into account that $dP_C/dr = dP_{\text{in}}/dr - dP_v/dr$, and

$$\begin{aligned} \frac{dP_C}{dr} &= -\frac{2\sigma}{r^2} \\ \frac{dP_v}{dr} &= -P_{fs} \frac{2\sigma v_L}{RT} \left(\frac{1}{r^2} \right) \exp\left(\frac{2\sigma v_L}{rRT} \right) \end{aligned} \quad (4)$$

we can evaluate the absolute values of the pressure variations of the system. Figure 1 shows the variation of the pressure for water as a function of droplet radius at 273.15 K, the external pressure being the same as the vapor pressure. In this figure, no significative differences between dP_C/dr and dP_{in}/dr are observed, even in the radius range where P_v/P_{fs} differs from unity ($r \lesssim 10$ nm).^{8,9} Moreover, this behavior persists (Figure 1b) even when considering the variation of the surface tension with radius by using the Tolman length $\delta(r) = \delta(1 + \delta/r + (1/3)\delta^2/r^2)$, (Figure 1).

* To whom correspondence should be addressed. E-mail: acastell@ivic.ve.

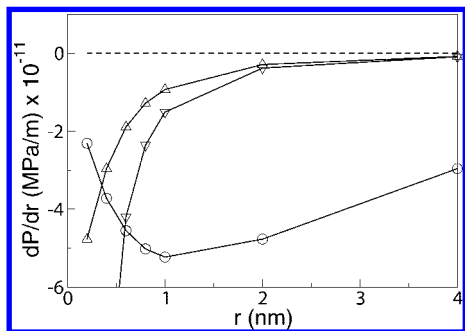


Figure 1. Variation of pressure for water droplets dispersed into its vapor at 273.15 K. (▽), (Δ), and (○) represent the variations in capillary pressure (dP_C/dr) for $\delta = 0$ (Laplace), $\delta = 2.5 \times 10^{-10}$ and $\delta = 2.5 \times 10^{-9}$, respectively. Dotted and solid lines represent dP_v/dr and dP_{in}/dr , respectively.

Based on the above considerations, we use the approximation $dP_{in}/dr \cong dP_C/dr$ since the absolute error estimated within this approximation is $\sim 5 \times 10^{-6}$ for radius larger than 10 nm and $\sim 2 \times 10^{-5}$ for $r \approx 1$ nm. This range of error is acceptable, taking into account that a radius of 1.2 nm corresponds to a cluster formed by a quite low number of molecules (~ 163).¹⁰

Now, let us consider the case of a gas bubble immersed into a liquid. To simplify the analysis let us assume that the gas is inert and insoluble and that an initial pressure P_{gas} is much higher than the liquid vapor pressure P_{fs} . The capillary pressure will be given by $P_C = P_{\text{in}} - P_{\text{out}}$, where P_{in} is the pressure inside the bubble. P_{in} has two contributions: the gas pressure and the vapor pressure of the liquid, that is, $P_{\text{in}} = P_{\text{gas}} + P'_v$. These quantities are related by the Kelvin equation for the case of concave curvature:

$$RT \ln \left(\frac{P'_v}{P_{\text{fs}}} \right) = - \frac{2\sigma v_L}{r} \quad (5)$$

This expression predicts that for any curvature radius $P'_v \leq P_{\text{fs}}$. However, a considerable change in the pressure of the liquid would be necessary in order to modify the vapor pressure ($P'_v < P_{\text{fs}}$). For the droplet in gas case, the liquid pressure P_{in} shows a sizable variation due to the curvature and leads to a modification of its vapor pressure, affecting the external pressure indirectly. For the bubble in the liquid case, an increment in pressure by curvature occurs in the gas phase as well as a contribution of the vapor pressure produced by the liquid. Meanwhile, the external phase is not affected. In other words, P_{out} is constant and therefore $P'_v = P_{\text{fs}}$. Following similar arguments we can also infer that in a liquid/liquid dispersion the change in pressure is produced by the effect of the curvature on P_{in} .

In this work we obtain an expression for the correction to σ due to the curvature of the disperse phase considering that the main contribution arises from P_{in} .

Dependence of the Surface Tension on the Curvature Radius of the Disperse Phase. In the above section, we have found that $dP_{in}/dr \cong dP_C/dr$ even in the range of curvature where P_v/P_{fs} and P'_v/P_{fs} differ from unity. This leads us to consider the problem starting from an initial system (A) where the total pressure is constant (see Figure 2). It is to say, the external pressure P_{out} for the gas in liquid system (B) and liquid in gas system (C) is considered to be constant.

Let us start by the Laplace equation:

$$P_{\text{in}} - P_{\text{out}} = \frac{2\sigma}{r} \quad (6)$$

Having in mind that P_{out} is not affected by the curvature radius, the variation with respect to r can be written as:

$$\frac{dP_{\text{in}}}{dr} = \frac{2}{r} \frac{d\sigma}{dr} - \frac{2\sigma}{r^2} \quad (7)$$

For solving eq 7 taking into account eq 6, one considers that the subindex “in” refers to the disperse phase and that the subindex “out” refers to the continuous phase. In addition, we introduce the assumption of equality between the chemical potentials corresponding to these two phases.

If we analyze the case of a liquid droplet immersed into a gas, the net variations of the chemical potentials of the phases in contact must be equal in order to maintain the equilibrium condition. Therefore, a variation in the curvature radius leads to an isothermal variation of the Gibbs potential of the liquid inside the droplet ($d\mu'$). This variation will be compensated by a variation in the surface Gibbs potential ($d\mu^\sigma$), that is,

$$d\mu_{\text{out}} = d\mu_{\text{in}} = d\mu^\sigma + d\mu' = 0 \quad (8)$$

Accordingly, we have:

$$d\mu' = -d\mu^\sigma \quad (9)$$

Isothermal variations of the Gibbs potentials are described by $d\mu' = (dP_{\text{in}})/(\gamma')$ and $d\mu^\sigma = \omega d\sigma = (\sigma)/(\Gamma)$. Then, from eq 9 we obtain $(\Gamma/\gamma')dP_{\text{in}} = -d\sigma$, or:

$$\delta' dP_{\text{in}} = -d\sigma \quad (10)$$

where $\delta' = \Gamma/\gamma'$. Combining eqs 7 and 10, we find the differential equation:

$$\left(1 + \frac{2\delta'}{r}\right) \frac{d\sigma}{dr} = \sigma \frac{2\delta'}{r^2} \quad (11)$$

Solving for σ we finally get:

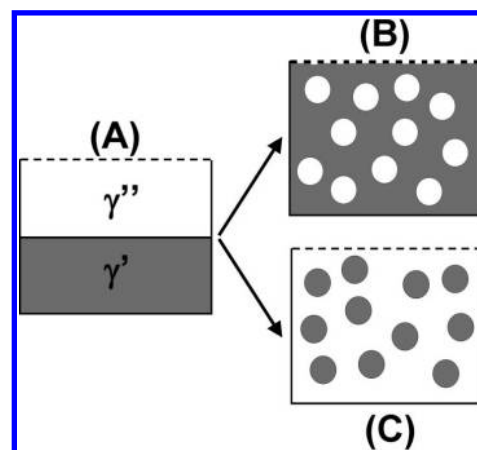


Figure 2. Starting liquid–gas system (A), and final systems as resulting from doing a work on (A): gas/liquid (B), or liquid/gas (C), at constant pressure (—).

$$\sigma = \sigma_{\infty} \left[\frac{1}{\left(1 + \frac{2\delta'}{r}\right)} \right] \quad (12)$$

Here, σ_{∞} refers to surface tension of a plane interface. Equation 12 has the same form to that obtained by Tolman (eq 4.3 in ref 2), but δ' differs from δ proposed by Tolman. For instance, δ' will never be negative or infinity. On the other hand, this equation can be derived to properly treat the situation where the internal phase has a lower density than the external one, that is, a gas bubble immersed into a liquid. In that case, the term $\delta'' = \Gamma/\gamma''$ will appear in eq 12 instead of δ' , and δ'' will never be negative or infinity. The terms δ' and δ'' are related to the geometrical conformation of the molecules in the fluid. This can be visualized considering a slab of volume Al , where $A = 1/\Gamma$ and l is the slab width. Three slabs having the same area and containing one mole defined in the liquid, interface and vapor phases, will have the width $l = \delta'$, Δ^{σ} , and δ'' , respectively, where Δ^{σ} is the interfacial width. The relationship between these parameters and the Tolman length, $\delta = \Gamma/(\gamma' - \gamma'')$, is:

$$\frac{1}{\delta} = \frac{1}{\delta'} - \frac{1}{\delta''} \quad (13)$$

Except near the critical point, δ'' is about 10^3 – 10^4 times δ' . In that case, from eq 13, we have $\delta \approx \delta'$. According to eq 12 one can expect that a decrease in the surface tension of a bubble immersed in a liquid should occur for larger radii than for the case of droplets immersed in a gas.

Unfortunately, there is no experimental measurements to be contrasted with the above results. Yet, we can consider the following isothermal variations with respect to the properties of the disperse phase (in):

$$\left(\frac{\partial \sigma}{\partial r}\right)_T = \left(\frac{\partial \sigma}{\partial \Gamma}\right)_T \left(\frac{\partial \Gamma}{\partial \gamma_{in}}\right)_T \left(\frac{\partial \gamma_{in}}{\partial P_{in}}\right)_T \left(\frac{\partial P_{in}}{\partial r}\right)_T \quad (14)$$

By a comparison with eq 10, we identify:

$$\delta_{in} = -\left(\frac{\partial \sigma}{\partial \Gamma}\right)_T \left(\frac{\partial \Gamma}{\partial \gamma_{in}}\right)_T \left(\frac{\partial \gamma_{in}}{\partial P_{in}}\right)_T \quad (15)$$

where δ_{in} fulfills the equation

$$\delta_{in} dP_{in} = -d\sigma \quad (16)$$

Finally, from eqs 7 and 16 we recover eq 12 with δ_{in} as a parameter instead of δ' . To test the thermodynamic consistency of Tolman as well as our deduction, we evaluate the behavior of δ_{in} for bubbles and droplets dispersions. This allows us to verify whether δ_{in} tends to an unique value, as Tolman proposed, or sizable differences exist between the values of δ_{in} for these two cases.

In order to evaluate eq 15, Γ can be considered as dependent on the dividing plane density γ_G according the relation $\Gamma = \kappa \gamma_G^{2/3}$, where κ is a constant that depends on the molecular projection model on the surface. In that case, the values of δ , δ' , and δ'' are proportional to κ . Besides, γ_G is considered to have a value between γ' and γ'' given by:

$$\gamma_G = m\gamma' + (1 - m)\gamma'' \quad (17)$$

where the parameter m is a fraction of unity.

To evaluate the term $(\partial \sigma / \partial \Gamma)_T$, we consider the isothermal changes in tension depending exclusively on the plane density Γ . Then it can be evaluated by means of the behavior of the saturation curves for pure fluids. In that case, $(\partial \sigma / \partial T)_{sat} = (\partial \sigma / \partial \Gamma)_T (\partial \Gamma / \partial T)_{sat}$, and:

$$\left(\frac{\partial \sigma}{\partial \Gamma}\right)_T = \frac{\left(\frac{\partial \sigma}{\partial T}\right)_{sat}}{\left(\frac{\partial \Gamma}{\partial \gamma_G}\right)_T \left[\left(\frac{\partial \gamma_G}{\partial \gamma'}\right) \left(\frac{\partial \gamma'}{\partial T}\right)_{sat} + \left(\frac{\partial \gamma_G}{\partial \gamma''}\right) \left(\frac{\partial \gamma''}{\partial T}\right)_{sat} \right]} \quad (18)$$

From eq 17 and $\Gamma = \kappa \gamma_G^{2/3}$, we can write:

$$\left(\frac{\partial \sigma}{\partial \Gamma}\right)_T = \frac{\left(\frac{\partial \sigma}{\partial T}\right)_{sat}}{\frac{2}{3} \kappa \gamma_G^{-1/3} \left[m \left(\frac{\partial \gamma'}{\partial T}\right)_{sat} + (1 - m) \left(\frac{\partial \gamma''}{\partial T}\right)_{sat} \right]} \quad (19)$$

Results

Systems composed by water droplets dispersed into methane gas and bubbles of methane dispersed into liquid water at atmospheric pressure and 273.15 K were considered. Methane gas was used to estimate the behavior of bubbles immersed into liquid water because experimental data for water vapor below the saturation pressure cannot be obtained. As it is known, methane gas is not soluble in water and also remains without phase change even for high pressures at 273.15 K.

The value of κ was adjusted to satisfy a surface area of 7016.28 m²/mol, that is, $\kappa = 2.5632 \times 10^{-6}$ for all cases. Due to the fact that Γ depends on the m value, then δ , δ' , and δ'' also depend on this parameter.

For the case of water droplets in methane gas, from eqs 15 and 17 we have:

$$\delta_{in} = -\left[m \left(\frac{2}{3} \kappa \gamma_G^{-1/3}\right) \left(\frac{\partial \sigma}{\partial \Gamma}\right) \left(\frac{\partial \gamma'}{\partial P_{in}}\right) \right]_T \quad (20)$$

To evaluate $(\partial \sigma / \partial \Gamma)_T$ using eq 19 we must determine $(\partial \sigma / \partial T)_{sat}$. The latter results from the general expression:

$$\sigma = B\Theta^{\eta}(1 + b\Theta) \quad (21)$$

where $\Theta = 1 - T/T_C$ and T_C is the critical temperature. For the case of water the values reported by Vargaftik et al.¹¹ are $B = 2.358 \times 10^{-3}$ N/m, $b = 0.625$, and $\eta = 1.256$. Using eq 21 we get:

$$\left(\frac{\partial \sigma}{\partial T}\right)_{sat} = -\frac{B}{T_C} \Theta^{\eta} \left(\frac{\eta}{\Theta} + b(\eta + 1) \right) \quad (22)$$

The procedure to estimate $(\partial \gamma' / \partial T)_{sat}$ and $(\partial \gamma'' / \partial T)_{sat}$ is shown in Appendix B. To evaluate $(\partial \gamma' / \partial P_{in})$ we used density values reported by Sato et al.¹²

For the bubble case, δ_{in} is given by:

$$\delta_{in} = - \left[(1 - m) \left(\frac{2}{3} \kappa \gamma_G^{-1/3} \right) \left(\frac{\partial \sigma}{\partial \Gamma} \right) \left(\frac{\partial \gamma''}{\partial P_{in}} \right) \right]_T \quad (23)$$

In the above equation, overheated methane data reported in Perry's book¹³ were used to obtain $(\partial \gamma'' / \partial P_{in})$.

Figures 3a and 3b show the dependence of δ_{in} on m for droplet and bubble cases, respectively. Notice that in a singular value of m ($m_s = 0.012254$) the function diverges. Let us stress that δ_{in} depends on m only, whereas δ' and δ'' depend on κ and m . As can be observed in Figure 3a, $\delta_{in} = \delta'$ for $m = 0.00667$. For the same value of m , it can be seen in Figure 3b that $\delta_{in} \approx \delta''$. A sizable difference between the values of δ_{in} for bubbles and droplets is found for the same value of m . In fact, δ_{in} for bubbles is approximately 10^3 – 10^4 times higher than δ_{in} for droplets, which is in agreement with the difference between the values of δ' and δ'' . This result supports the deduction proposed in this work.

The singular value m_s shown in Figure 3 is the same for bubble and droplet. This results from the divergent term $(\partial \sigma / \partial \Gamma)_T$, which appears in eqs 20 and 23. The divergence of this term occurs when the denominator appearing in the second factor of eq 19 vanishes, that is, when

$$m \left(\frac{\partial \gamma'}{\partial T} \right)_{sat} + (1 - m) \left(\frac{\partial \gamma''}{\partial T} \right)_{sat} = 0 \quad (24)$$

this equation determining $m = m_s$. From the shape of the function δ_{in} appearing in Figure 3 it can be seen that the dependence of σ on Γ will correspond to a decrease of σ when Γ increases only for $m < m_s$. Therefore, m_s may be considered as the limit of m beyond which the dependence of σ on Γ becomes nonphysical. On the other hand, m_s changes with temperature, as can be seen in Figure 4a. The dependence of m_s with T appearing in Figure 4a indicates that m_s tends to 0.5 when approaching the critical point ($T = T_C$), which is in agreement with the uniformity between gas and liquid phases occurring at this temperature. The results illustrated in this figure

and the dependence of γ_G as a function of m_s given by eq 17 suggest that the interface consists of an expanded liquid, with the interfacial energy being mainly accumulated in the liquid phase. In previous works we arrive to an analogous conclusion by following a different approach.^{14,15} This effect is more pronounced near the fusion point. This is in agreement with the experimental fact that the surface tension of water at 298.15 K and low pressure is ≈ 0.072 N/m, no matter what gas is in contact with the liquid. Also, as the temperature rises, the interfacial plane will be located at an intermediate position between the phases (Figure 4a). In Figure 4b the values of Γ calculated for $m = m_s$ are shown. On the other hand, the slow change of Γ with m implies that the real values of Γ for any temperature should be closer to $\Gamma(m_s)$. Moreover, the behavior of Γ seems to be independent of a critical exponent, unlike the gas and liquid densities, since it grows monotonously from above 350 K.

Figure 5 shows differences in the change of surface tension with the curvature radius for the water/gas-methane and gas-methane/water systems. According to these results, the internal pressure P_{in} in droplets is higher than in bubbles for the same curvature radius. Besides, surface tension diminishes abruptly for bubbles smaller than 100 μm , whereas for droplets sizable changes in tension are observed only in the size range of 1–10 nm.

In Figure 6, changes in Γ for droplets and bubbles systems are illustrated. In all cases, Γ changes with the curvature radius. An increment in internal pressure generates a variation in the fluid density confined into the spheres corresponding to the disperse phase. As the curvature radius decreases, we identify the increment in the surface density Γ as one of the mechanisms by which the system diminishes the surface tension. It is to say, for the droplet case, the dividing spherical surface of tension displaces toward the center. In contrast, for the bubble case, the spherical surface of tension displaces out from the center.

It can be observed in Figure 6 that the variation of Γ happen at the same radius value where the tension starts to diminish

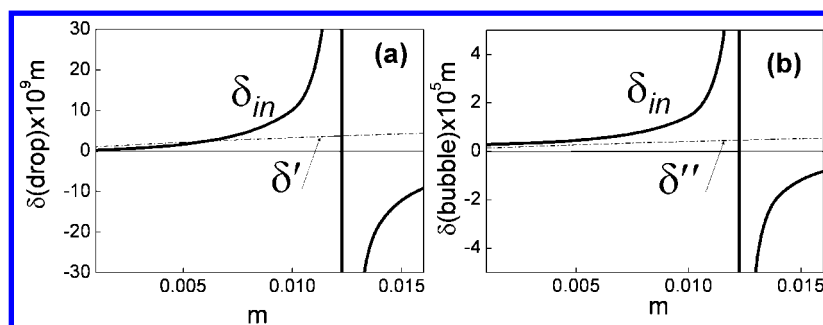


Figure 3. Characteristic lengths δ for droplet/gas (a) and bubble/liquid systems (b).

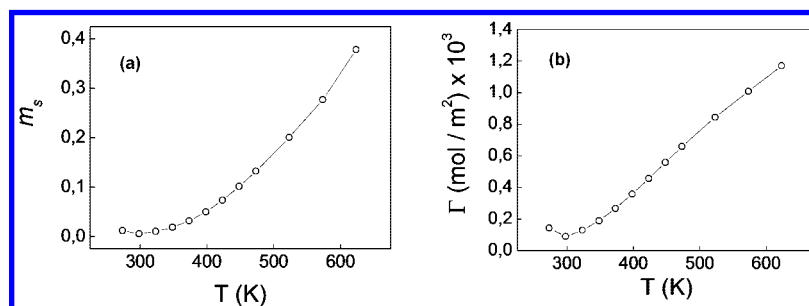


Figure 4. Singular points (m_s) for saturated water with its vapor from fusion point to near the critical point (a). Surface densities (Γ) determined in those points using an arbitrary $\kappa = 2.5632 \times 10^{-6}$ (b).

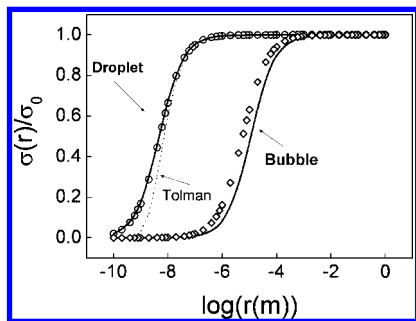


Figure 5. Surface tension by considering the Tolman length (—), δ' for droplets (○) and δ'' for bubbles (◇). δ_{in} for droplets and bubbles is also represented (···). $m = 0.00667$ in all cases.

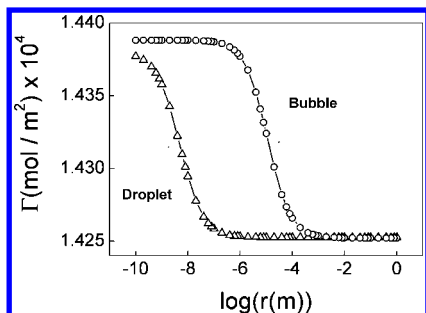


Figure 6. Surface density behavior Γ with curvature radius, for bubbles (—○—) and droplets (—Δ—).

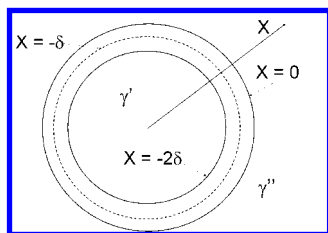


Figure 7. Location of surfaces describing the interface of a spherical particle.

TABLE 1: Polynomial Coefficient Values of Equations 31 and 32

N'_0	1.9332×10^{-6}	N''_0	$-2.9489 \times 10^{-8} \text{ K}^{-1}$
N'_1	1.9575	N''_1	-2.1302
N'_2	-0.6607	N''_2	-5.6483
N'_3	6.3146×10^{-4}	N''_3	3.3286
N'_4	-0.9506	N''_4	-3.1486
		N''_5	-2.7804

(see Figure 5). By using a representation of σ/σ_0 as a function of $(\Gamma(r) - \Gamma(0))/(\Gamma(\infty) - \Gamma(0))$ we obtain a linear correlation with $R^2 \cong 1$ for both droplets and bubbles cases. This leads us to an approximate relation between $\sigma(r)$ and $\Gamma(r)$, given by:

$$\frac{d\sigma(r)}{dr} \cong \frac{\sigma(\infty) - \sigma(0)}{\Gamma(\infty) - \Gamma(0)} \frac{d\Gamma(r)}{dr} \quad (25)$$

where $\Gamma(0) = \lim_{r \rightarrow 0} \Gamma(r)$. According to eq 12 the main variation of σ comes from its dependence on r . Yet, the appearance of δ' or δ'' in the terms $2\delta'/r$ or $2\delta''/r$ in eq 12 introduces a dependence of σ on Γ since $\delta' = \Gamma(r)/\gamma'$ and $\delta'' = \Gamma(r)/\gamma''$. On the other hand, $\Gamma(r)$ increases as the radius r diminishes (see Figure 6). Then, the variation of $\Gamma(r)$ with r will tend to enhance the dependence of σ on r .

The increments in Γ when the radius decreases shown in Figure 6 are small compared with the dependence in curvature

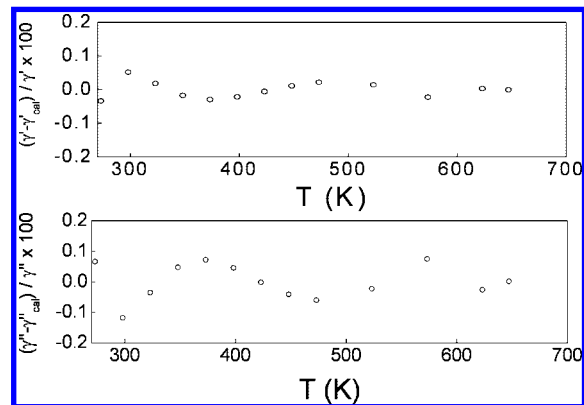


Figure 8. Absolute deviations of calculated densities from the experimental data.¹²

radius proposed by Tolman. Accordingly, we see in Figure 5 that by using the Tolman proposal, one obtains that the surface tension has a more abrupt variation than that obtained by our procedure.

Conclusions

(1) According to our analysis, the gas/liquid dispersions show variations in surface tension with curvature radius different from those predicted for the liquid/gas dispersions. In particular, one can expect that a decrease in the surface tension of a bubble immersed in a liquid when the curvature radius decreases should occur for much larger radii than for the case of droplets immersed in a gas.

(2) The increment of the surface density Γ , was identified as one of the possible mechanism contributing to lowering the surface tension as curvature radius decreases.

(3) The dependence of γ_G as a function of temperature suggests that the interfacial energy is mainly accumulated in the liquid phase for a wide range of temperature.

Appendix

Appendix A.

The relationship between the Tolman length $\delta = \Gamma/(\gamma' - \gamma'')$ and the interfacial width of a spherical surface can be derived directly. Let us consider that $x = 0$ is located at the more external spherical surface of the droplet. Analogously, we can define an internal shell located at -2δ from $x = 0$ to the center, as shown in Figure 7. Between these surfaces all the interfacial phenomena occur.

Surface density behavior in this region can be simplified as follows:

$$\gamma = \begin{cases} \gamma' & \text{if } x \leq -2\delta \\ \bar{\gamma} & \text{if } x = -\delta \\ \gamma'' & \text{if } x \geq 0 \end{cases} \quad (26)$$

with $\bar{\gamma} = \int_{-2\delta}^0 \gamma(x)(1 + cx)^2 dx / 2\delta$. Then, we have:

$$\Gamma = \int_{-2\delta}^0 (\gamma - \gamma')(1 + cx)^2 dx + \int_{-\delta}^0 (\gamma - \gamma'')(1 + cx)^2 dx \quad (27)$$

where $c = 1/r$. Integrating we obtain:

$$\Gamma = (\gamma - \gamma')x(1 + cx + (1/3)c^2x^2) \Big|_{-2\delta}^{-\delta} + (\gamma - \gamma'')x(1 + cx + (1/3)c^2x^2) \Big|_{-\delta}^0 \quad (28)$$

which leads to:

$$\Gamma = (\bar{\gamma} - \gamma')(-\delta)(1 - c\delta + (1/3)c^2\delta^2) - (\bar{\gamma} - \gamma'')(-\delta)(1 - c\delta + (1/3)c^2\delta^2) \quad (29)$$

$$\Gamma = (\gamma' - \gamma'')\delta(1 - c\delta + (1/3)c^2\delta^2) \quad (30)$$

For a plane surface, $\lim_{r \rightarrow \infty} c \rightarrow 0$ and $\Gamma/(\gamma' - \gamma'') \rightarrow \delta$. Then, it can be inferred that the Tolman length is related to the interfacial width Δ^o according to $\Delta^o \approx 2\delta$.

Appendix B.

To estimate $((\partial\gamma')/(\partial T))_{\text{sat}}$ and $((\partial\gamma'')/(\partial T))_{\text{sat}}$, the proposed procedure correlates γ' and γ'' with temperature throughout the saturation curve. Let us define the variables $\rho' = \ln(\gamma'/\gamma_c)$ and $\rho'' = \ln(\gamma''/\gamma_c)$, where γ_c is the water density at the critical point.

It has been found that ρ' and ρ'' are in good agreement with experimental data when they are expressed as:

$$\rho' = [N'_0 + N'_1\Theta^{1/3} + N'_2\Theta^{2/3} + N'_3\Theta^{8/3} + N'_4\Theta^{35/6}] \quad (31)$$

$$\rho'' = \frac{T_c}{T} [N''_0T + N''_1\Theta^{1/3} + N''_2\Theta^{5/6} + N''_3\Theta^{7/6} + N''_4\Theta^{14/3}] \quad (32)$$

where $\Theta = 1 - T/T_c$ and T_c is the critical temperature of water.

Figure 8 illustrates the absolute deviations of calculated densities from the experimental data. They are smaller than 0.1%. The polynomial coefficients of 31 and 32 are given in Table 1.

Finally, we obtain the quantities $((\partial\gamma')/(\partial T))_{\text{sat}}$ and $((\partial\gamma'')/(\partial T))_{\text{sat}}$ from

$$\left(\frac{\partial\gamma'}{\partial T}\right)_{\text{sat}} = \gamma' \left(\frac{\partial\rho'}{\partial T}\right)_{\text{sat}} \quad (33)$$

and

$$\left(\frac{\partial\gamma''}{\partial T}\right)_{\text{sat}} = \gamma'' \left(\frac{\partial\rho''}{\partial T}\right)_{\text{sat}} \quad (34)$$

Acknowledgment. This work was financially supported by FONACIT Grant G-2005000418. We thank Carlos Toro and Monica Garcia-Nustes for their help on the manuscript preparation.

References and Notes

- (1) Mason, T. G.; Graves, S. M.; Wilking, J. N.; Lin, M. Y. *J. Phys. Chem. B* **2006**, *110*, 22097.
- (2) Tolman, R. J. *Chem. Phys.* **1949**, *17*, 333.
- (3) Lei, Y. A.; Bykov, T.; Yoo, S.; Zeng, X. C. *J. Am. Chem. Soc.* **2005**, *127*, 15346.
- (4) Lu, H. M.; Jiang, Q. *Langmuir* **2005**, *21*, 779.
- (5) Onischuk, A. A.; Purto, P. A.; Baklanov, A. M.; Karasev, V. V. *J. Chem. Phys.* **2006**, *124*, 014506.
- (6) Koga, K.; Zeng, X. C.; Shchekin, A. K. *J. Chem. Phys.* **1998**, *109*, 4063.
- (7) Iwamatsu, M. *J. Phys.: Condens. Matter* **1994**, *6*, L173.
- (8) Fisher, L. R.; Gamble, R. A.; Middlehurst, J. *Nature* **1981**, *290*, 575.
- (9) Mitropoulos, A. C. *J. Colloid Interface Sci.* **2008**, *317*, 643.
- (10) Dobruskin, V. K. *Langmuir* **2003**, *19*, 4004.
- (11) Vargaftik, N. B.; Volkov, B. N.; Voijak, L. D. *J. Phys. Chem. Ref. Data* **1983**, *12*, 817.
- (12) Sato, H.; Uematsu, M.; Watanabe, K.; Saul, A.; Wagner, W. *J. Phys. Chem. Ref. Data* **1988**, *17*, 1439.
- (13) Perry, R. H.; Green, D. W.; Maloney, J. O. *Manual del Ingeniero Químico*; McGraw-Hill: 1992.
- (14) Castellanos, A. J.; Urbina-Villalba, G.; Garcia-Sucre, M. *J. Phys. Chem. B* **2003**, *108*, 5951.
- (15) Castellanos, A. J.; Urbina-Villalba, G.; Garcia-Sucre, M. *J. Phys. Chem. B* **2006**, *110*, 2751.

JP808906P